

Hyperspectral Face Recognition Using 3D Gabor Wavelets

Linlin Shen and Songhao Zheng

School of Computer Science and Software Engineering

Shenzhen University, China

llshen@szu.edu.cn

Abstract

Compared to the fruitful research outputs in 2D face recognition, the research in hyperspectral face recognition is quite limited in literature. When most available works process 2D slices of hyperspectral data separately, a 3D Gabor wavelet based approach is proposed in this paper to extract features in spatial and spectrum domain simultaneously. As a result, the information contained in the 3D data can be fully exploited. Experimental results show that the proposed approach substantially outperforms the methods available in literature such as spectrum feature, PCA and 2D-PCA on the HK-PolyU Hyperspectral Face Database under the same testing protocol. When only one sample per subject is available for training, our method also achieves very robust performance.

1. Introduction

Since 1970s, a large number of face recognition technologies have been developed in literature, which can mainly be classified into two categories, i.e. global and local approaches [1]. Though high accuracy has been achieved for frontal view face images captured in controlled environment, large illumination, pose variations and time remain great challenges to current face recognition technologies.

While hyperspectral imaging has been widely used to space and airborne imaging for remote sensing applications, it was not introduced to face recognition until recently, due to the high cost of imaging device. Pan et al. [2] extract the mean spectral signatures of sampled face regions at forehead, cheek and mouth for recognition. The method was tested using the hyperspectral face images collected from 200 subjects with pose and expression variations. The results show that the performance is robust against such variations. Their more recent work [3] extended the previous study with constant illumination, and unknown outdoor illumination was introduced. Again robust

performance was observed. As hyperspectral data usually contain tens of 2D images captured at different spectral bands, some researchers performed recognition on each 2D image and then fused these results for final decision. The commercial FaceIt software and different fusion schemes were tested in Chang et al.'s work [4]. They observed that when different illuminations like halogen, fluorescent and day light are present, hyperspectral face images achieve more robust performance than conventional methods using visible lights. Similarly, 2D PCA and decision level fusion were adopted in Di et al's work [5]. Since most current approaches in literature either use spectrum signature, or feature extracted from spatial domain only for recognition, the rich amount of information included in hyperspectral data is not fully explored. The work in [6] tries to perform joint spatial-spectrum analysis by sampling the pixel values of different bands to generate a so-called 2D spectral-face image. When the same eigenface technique was applied, the spectral-face method achieves better performance than that using single band and multi-band face images. However, the sampling of pixels was ad hoc. When only few samples at different bands are randomly included, lots of useful information is lost.

Compared with the fruitful researches done in face recognition using visible light, the work in hyperspectral face recognition is quite limited. We first propose in this paper a 3D Gabor wavelet based approach for hyperspectral face recognition. When spatial-spectrum relationships are jointly analyzed by Gabor wavelets with different central frequencies, the information included in hyperspectral data can be fully explored. The method was tested using the publicly available HK-PolyU Hyperspectral Face Database [13] and remarkable improvements over previous results have been observed.

2. 3D Gabor Wavelet Representation for Hyperspectral Face Data

2.1. 3D Gabor wavelets

The Gabor function [7] was proposed to maximize the resolution for joint time and frequency analysis of signals, which is a Gaussian modulated by a sinusoidal function. The 2D counterpart of a Gabor elementary function was first introduced by Granlund [8]. Since then, 2D Gabor wavelet has been widely applied to extract features for texture classification [9, 10], palmprint recognition [11] and face recognition [1], etc. In spatial-spectrum domain (x,y,b) , the 3D Gabor wavelets can be defined as below [12]:

$$\left\{ \begin{array}{l} \Psi_{f,\varphi,\theta}(x,y,b) = S \times \exp\left[-\left(\frac{x'}{\sigma_x}\right)^2 + \left(\frac{y'}{\sigma_y}\right)^2 + \left(\frac{b'}{\sigma_b}\right)^2\right] \times \exp(j2\pi(xu + yv + bw)) \\ u = f \sin \varphi \cos \theta, \quad v = f \sin \varphi \sin \theta, \quad w = f \cos \varphi \\ [x' \ y' \ b']^T = R \times [x - x_c \ y - y_c \ b - b_c]^T \end{array} \right. \quad (1)$$

where S is a normalization scale, (x_c, y_c, b_c) is the position for signal analysis, f is the central frequency of the sinusoidal plane wave, φ and θ are the angles of the wave vector with w axis and $u-v$ plane in frequency domain (u,v,w) , R defines the rotation matrix for transforming the Gaussian envelope to coincide with orientation of the sinusoid, and $\sigma_x, \sigma_y, \sigma_b$ are the width of Gaussian envelop in different axis. The response of signal to wavelet $\Psi_{f,\varphi,\theta}$ represents the strength of variance with frequency amplitude f and orientation (φ, θ) . Figure 1 shows the real components of two example 3D Gabor wavelets in spatial-spectrum domain with different orientations and frequencies.

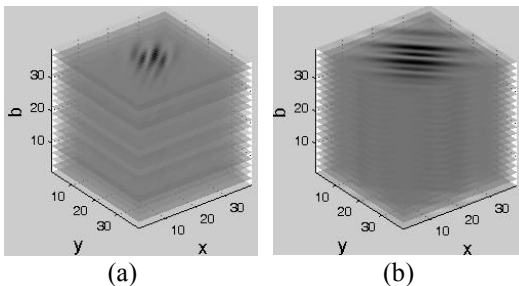


Figure 1. Two example 3D Gabor wavelets in spatial-spectrum domain

Since local information about frequency and orientation are usually unknown, a family of $I \times J \times K$

Gabor wavelets with different frequencies is required to extract features from volume data:

$$\left\{ \Psi_{f_i, \varphi_j, \theta_k}(x, y, b), \quad f_i = \frac{f_{\max}}{(2)^i}, \quad \varphi_j = j\pi/J, \quad \theta_k = k\pi/K \right\} \quad (2)$$

where $f_i, (\varphi_j, \theta_k)$ define the amplitude and orientations of central frequency, f_{\max} is the highest possible amplitude of frequency, 2 (one octave) is the spacing factor between different scales. The frequency vector points to the same direction with different θ when $\varphi=0$. In this paper, we simplify the representation of the wavelets and denote them as $\{\Psi_{ij,k}, i=0,1,\dots,I-1; j=0,1,\dots,J-1; k=0,1,\dots,K-1\}$. While the inner product of signal with wavelet set $\{\Psi_{ij,k}\}$ at location (x_c, y_c, b_c) represents information about local signal variances. The convolution results include such information at all possible locations in space-spectrum domain (x,y,b) .

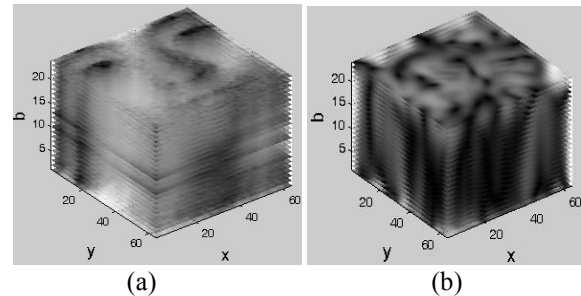


Figure 2. (a) An example of hyperspectral face cube and (b) its Gabor transform.

2.2. Feature Extraction

Given a set of 3D Gabor wavelets $\{l, l=1,2,\dots,L\}$ and a hyperspectral face image $V(x,y,b)$, where (x,y) represents the spatial coordinates in space domain and b denotes the wavelength of spectral band, the convolution result contains important information about signal variances in the hyperspectral data V . Figure 2 shows an example of hyperspectral face image volume and its convolution result with the 3D Gabor wavelet shown in Figure 1(a). While the face cube shows variations across both spatial and spectral domains, the magnitude of convolution output reflects the strength of such variations. The coefficient $G_l(x,y,b)$ extracted at location (x,y,b) in the spatial-spectrum domain contains important information about local signal variations in the frequency of applied Gabor wavelet. To include all local information, a feature vector X_l can be generated by concatenating the magnitude of convolution outputs at different locations:

$$X_l = \left[|G_l(0,0,0)| \cdots |G_l(x,y,b)| \cdots |G_l(W-1,H-1,B-1)| \right] \quad (3)$$

where W and H are the width and height of face image in space domain, B is the number of spectrum bands. The dimension of feature generated by wavelet l is thus $W \times H \times B$. Similar to wavelet analysis, the feature extracted by all L wavelets can be combined as:

$$X = [X_1 \cdots X_l \cdots X_L] \quad (4)$$

3. Experimental Results

3.1. Dataset

The publicly available HK-PolyU Hyperspectral Face Database [13] is used in the experiments for testing. To get multi-spectrum data, a CRI's VariSpec LCTF was used to filter the light with wavelength less than 400nm and greater than 720nm [5]. With a step length of 10nm, the spectral range produces 33 bands in all. The face images were captured from 48 young volunteers (13 females and 35 males) at different sessions. In each session, frontal hyperspectral face samples with neutral expression were collected for each subject. While at least 4 sessions were collected for the first 25 subjects, one or two sessions are available for the remaining individuals. The eye coordinates were manually located and each face was cropped and rotated with reference to the eye locations and resized to size 64×64 . Figure 3 shows the first 32 bands of an example hyperspectral face. The 33rd band was not included in the figure due to the space reason.



Figure 3. The first 32 bands of an example hyperspectral face image.

3.2. Results

The testing protocol described in [5] was adopted here. In this protocol, 25 subjects with 4 data cubes of frontal hyperspectral face images available are selected for testing. For each subject, two of the four cubes were randomly selected as gallery and the remaining two were used as probe. The process was repeated 6 times and the average accuracy was recorded. To keep

the same settings as [5], the first six and last three bands, as shown in Figure 4, were removed due to high noise, leaving 24 spectral bands in total. As a result, the results reported in [5] are directly comparable with our method.



Figure 4. The removed nine bands

We first test the performance of the proposed Gabor features using 52 wavelets according to Eq. (3). In this paper, we set $f_{max}=0.25$, $I=J=K=4$. A set of 52 wavelets $\{\Psi_l, l=1,2,\dots,52\}$ could thus be produced for feature extraction. The frequency f takes the amplitudes of $[0.25, 0.125, 0.0625, 0.03125]$ with φ and θ set as the values of $[0, \pi/4, \pi/2, 3\pi/4]$, respectively. After convolution with the hyperspectral face, each wavelet Ψ_l could contribute a feature X_l with dimension $64 \times 64 \times 33 = 135,168$ when 33 bands were used. The 52 features extracted by different Gabor wavelets were tested individually and accuracy of the best one was recorded.

All of the 52 features X_l generated by individual Gabor wavelets were then combined to a single feature vector (see Eq. (4)) to represent signal variances at different scales and orientations. The dimension of feature vector is thus 52 times that of X_l , which is already very high. Downsampling is first used to reduce the dimension of feature vector for computation and memory efficiency. We tested different downsampling rates in both spatial and spectrum domain. Considering both accuracy and efficiency, we choose 4 and 3 as the rate in spatial domain and spectrum domain, respectively. The dimension of combined Gabor feature can thus be greatly reduced.

To make a comparison with other methods in literature, we also implemented the spectrum features used in references [2], [3] and the spectral Eigenface proposed in [6]. The commercial face recognition software used in [4] is not available for testing in this paper. For spectrum feature, four facial regions corresponding to forehead, left cheek, right cheek and lips were used. For spectral Eigenface, the value of pixel i in spectral-face was assigned as the value of corresponding pixel in band b , which is the remainder of i divided by number of bands.

The performances of the proposed 3D Gabor feature based methods and these approaches in literature, are listed in Table 1. Though spectrum feature was reported to achieve robust performance in [2] and [3], where hyperspectral data were collected over the near-infrared (0.7-1.0 μ m), its performance in

this test is not satisfactory for hyperspectral data collected in visible spectrum (0.4-0.72 μ m). Due to the incorporation of spatial information, both spectral Eigenface and 2D PCA improve the accuracy to above 70%. When the individual Gabor feature achieved 82% accuracy, the combined Gabor feature substantially improves the performance to as high as 91.3% (std: 2.42%). The performance proves the effectiveness of 3D Gabor wavelets for feature representation in joint spatial-spectral domain. Note that the best individual Gabor feature was extracted using wavelet with frequency 0.0625 and orientation ($3\pi/4, 3\pi/4$).

TABLE 1. PERFORMANCES

<i>Method</i>	<i>Accuracy</i>
Spectrum Feature [2] [3]	45.35%
Spectral Eigenface [6]	70.33%
Fusion of 2D PCA [5]	79.00%
Best Individual 3D Gabor	82.00%
Combined 3D Gabor	91.30%

4. Conclusions

In this paper we proposed a 3D Gabor wavelet based approach for hyperspectral face recognition. As a comparatively new research area, the works done in

References

- [1] L. Shen and L. Bai, "A review on Gabor wavelets for face recognition," *Pattern Analysis and Applications*, vol. 9, pp. 273-292, 2006.
- [2] Z. Pan, G. Healey, M. Prasad, and B. Tromberg, "Face recognition in hyperspectral images," *IEEE Transactions on Pattern Analysis and Machine Intelligence*, vol. 25, pp. 1552-1560, 2003.
- [3] Z. Pan, G. Healey, and B. Tromberg, "Hyperspectral face recognition under unknown illumination," *Optical Engineering*, vol. 46, pp. 077201, 2007.
- [4] H. Chang, A. Koschan, B. Abidi, and M. Abidi, "Fusing continuous spectral images for face recognition under indoor and outdoor illuminants," *Machine Vision and Applications*, vol. 21, pp. 201-215, 2010.
- [5] W. Di, L. Zhang, and D. Zhang, "Studies on hyperspectral face recognition in visible spectrum with feature band selection," *IEEE Transactions on Systems, Man and Cybernetics, Part A*, vol. 40, pp. 1354-1361, 2010.
- [6] Z. Pan, G. Healey, and B. Tromberg, "Comparison of spectral-only and spectral/spatial face

recognition is quite limited so far. When most of the works in literature separately process the images captured with different light bands, our approach jointly processes the data in spatial-spectrum and frequency domains. The extracted 3D Gabor features thus contains useful information about facial features cross both space and spectrum domains.

Experiments were conducted using a publicly available hyperspectral face database captured at the Hong Kong Polytechnic University. When the same testing protocol was used, the proposed approach substantially outperforms the method developed in literature such as spectrum feature, PCA and 2D PCA, which fuses the features extracted from selected bands. We are currently working on selecting the most useful bands for possible accuracy and efficiency improvement.

Acknowledgement

Work supported by National Natural Science Foundation of China (60903112), the Science Foundation of Shenzhen City (JC201104210035A) and the Open Research Fund of State Key Laboratory of Information Engineering in Surveying, Mapping and Remote Sensing (11R02).

- recognition for personal identity verification," *EURASIP Journal on Advances in Signal Processing*, vol. 2009, pp. 1-6, 2009.
- [7] D. Gabor, "Theory of communications," *Journal of Institution of Electrical Engineers*, vol. 93, pp. 429-457, 1946.
- [8] G. H. Granlund, "Search of a general picture processing operator," *Computer Graphics and Image Processing*, vol. 8, pp. 155-173, 1978.
- [9] F. Bianconi and A. Fernandez, "Evaluation of the effects of Gabor filter parameters on texture classification," *Pattern Recognition*, vol. 40, pp. 3325-3335, 2007.
- [10] M. Li and R. C. Staunton, "Optimum Gabor filter design and local binary patterns for texture segmentation," *Pattern Recognition Letters*, vol. 29, pp. 664-672, 2008.
- [11] D. Zhang, A. Kong, J. You, and M. Wong, "Online palmprint identification," *IEEE Transactions on Pattern Analysis and Machine Intelligence*, vol. 25, pp. 1041-1050, 2003.
- [12] L. Shen and L. Bai, "3D Gabor wavelets for evaluating SPM normalization algorithm," *Medical Image Analysis*, vol. 12, pp. 375-383, 2008.
- [13] "PolyU Hyper-spectral Face Database," 2010.